Using Deep Learning for estimation of river surface elevation from photogrammetric Digital Surface Models

Radosław Szostak
AGH UST
rszostak@agh.edu.pl

Marcin Pietroń
AGH UST
pietron@agh.edu.pl

Mirosław Zimnoch
AGH UST
zimnoch@agh.edu.pl

Przemysław Wachniew
AGH UST
wachniew@agh.edu.pl

Paweł Ćwiąkała
AGH UST
pawelcwi@agh.edu.pl

Edyta Puniach
AGH UST
epuniach@agh.edu.pl

Abstract

Development of the new methods of surface water observation is crucial in the perspective of increasingly frequent extreme hydrological events related to global warming and increasing demand for water. Orthophotos and digital surface models (DSMs) obtained using UAV photogrammetry can be used to determine the Water Surface Elevation (WSE) of a river. However, this task is difficult due to disturbances of the water surface on DSMs caused by limitations of photogrammetric algorithms. In this study, machine learning was used to extract a WSE value from disturbed photogrammetric data. A brand new dataset has been prepared specifically for this purpose by hydrology and photogrammetry experts. The new method is an important step toward automating water surface level measurements with high spatial and temporal resolution. Such data can be used to validate and calibrate of hydrological, hydraulic and hydrodynamic models making hydrological forecasts more accurate, in particular predicting extreme and dangerous events such as floods or droughts. For our knowledge this is the first approach in which dataset was created for this purpose and deep learning models were used for this task. Additionally, neuroevolution algorithm was employed to explore different architectures to find optimal models. The obtained results have better accuracy compared to manual methods of determining WSE from photogrammetric DSMs.

1 Introduction

Reports from international organizations indicate increasingly significant problems with earths water resources. The global demand for freshwater continues to increase at rate 1% per year since 1980s driven by population growth and socioeconomic changes. Simultaneously, the increase in evaporation caused increasing temperatures leads to a decrease in streamflow volumes in many areas of the world, which already suffer from water scarcity problems. Climate warming is also responsible for globally increased frequency of extreme hydrologic conditions. More intense and frequent precipitation events increase the flood risk as well as heatwaves are becoming more common and last longer, resulting in more severe droughts (UNESCO [2020], IPCC [2015]). Achieving socioeconomic and environmental sustainability under such challenging conditions will require the use of monitoring tools that will facilitate the management of the water resources. Traditional surface water management practices are primarily based on data collected from networks of in situ hydrometric gauges. Point measurements do not provide sufficient spatial resolution to comprehensively characterize river networks, and many developing regions lack them altogether. Moreover, the decline of existing measurement networks is

Fourth Workshop on Machine Learning and the Physical Sciences (NeurIPS 2021).

Table 1: Remote sensing small river WSE measurement error comparison. RMSE values taken from: UAV – Bandini et al. [2020], AIRSWOT – Altenau et al. [2017]

Method	RMSE (m)
UAV RADAR	0.03
AIRSWOT	0.09
UAV SfM DSM centerline	0.164
UAV SfM point cloud	0.180
UAV LIDAR point cloud	0.22
UAV SfM DSM "water-edge"	0.450

being observed all over the world (Lawford et al. [2013]). Remote sensing methods are considered as a solution to cover data gaps specific to point measurement networks (McCabe et al. [2017]). A leading example of remote sensing is measurements made from satellites. However, due to too low spatial resolution, satellite data is suitable only for studying the largest rivers. E.g. SWOT mission allows only observation of rivers of width greater than 50-100 m (Pavelsky et al. [2014]). In this regard, measurement techniques based on Unmanned Aerial Systems (UASs) are promising for small river measurements in many key aspects, as they are characterized by high spatial and temporal resolution, simple and fast deployment, and the ability to be used in inaccessible locations (Vélez-Nicolás et al. [2021]). Spatialy distributed Water Surface Elevation (WSE) measurements are highly important, as they are used for validation and calibration of hydrologic, hydraulic or hydrodynamic models to make hydrological forecasts, including predicting dangerous events such as floods and droughts (Langhammer et al. [2017], Tarpanelli et al. [2013], Jarihani et al. [2013], Domeneghetti [2016], Montesarchio et al. [2014])

Photogrammetric Structure from Motion (SfM) algorithms are able to generate Orthophotos and Digital Surface Models (DSMs) of terrain based on multiple aerial photographs. Photogrammetric DSMs are precise in determining the elevation of solid surfaces to within a few cm (Ouédraogo et al. [2014], Bühler et al. [2017]). However, they do not correctly represent the water surface. This is related to the fact that general principle of SfM algorithms is based on automatic search for a distinguishable and static terrain points that appear in several images showing these points from different perspectives. The surface of the water lacks such points as it is uniform, transparent and in motion. Due to water transparency, DSMs created using SfM algorithms typically indicate pixel elevations below the actual water surface level. For very clear and shallow streams, photogrammetric DSMs represent the river bottom (Kasvi et al. [2019]). For opaque waters, photogrammetric DSMs are disturbed by artifacts caused by water uniformity (lack of distinguishable photogrammetric key-points). Woodget et al. [2014], Javernick et al. [2014] and Pai et al. [2017] demonstrated that it is possible to read the WSE from photogrammetric DSM at shorelines ("water-edge") where river is very shallow, so there are no undesirable effects associated with light penetration below the water surface. However, Bandini et al. [2020] proved that this method gives satisfactory results only for unvegetated and smoothly sloping shorelines where the boundary line between water and land is easy to define. For this reason, this method is not suitable for universal automation. Table 1 shows the RMSE errors of existing Remote Sensing methods for measuring water levels in small rivers.

The aim of this work was to develop a new automatic method based on deep neural networks allowing estimation of small rivers WSE from photogrammetric DSMs and Orthophotos with an accuracy outperforming previous methods based on manual analysis of photogrammetric data.

2 Dataset

A brand new dataset has been prepared for the purpose of this work. It consists of 260 samples, each corresponding to a 10 by 10 meter area that encloses small river water body and nearshore land. Subjected rivers have width ca. 2-3 m. They are overhung by sparse deciduous trees. The banks and riverbed are overgrown with rushes that protrude above the water surface. The banks are steeply sloping at angles of ca. 50° to 90° relative to the water surface. Data were collected during different seasons, so individual samples differ in vegetation stage. There are marshes nearby, with river water flowing into them in places. Additionally, the dataset was supplemented with photogrammetric data from surveys made by Bandini et al. [2019]. See the cited publication for details on this river case study: Bandini et al. [2020]. Dataset samples were divided into a training and testing subset at a ratio of 8:2. Dataset is available to download at `https://doi.org/10.5281/zenodo.5257183` (Szostak et al. [2021]). Every sample includes:

- **Photogrammetric orthophoto**. Raw photogrammetric data. True color image represented as a $3 \times 256 \times 256$ array (3 channel image of 256×256 pixels).
- **Photogrammetric DSM**. Raw photogrammetric data. Contains disturbed water surfaces. Corresponds to the area presented on the orthophoto. Stored as a 256×256 array containing elevations of pixels expressed in m MSL.
- **WSE**. Ground truth Water Surface Elevation as single value expressed in m MSL.
- **Photogrammetric DSM statistics**. Mean, standard deviation, minimum and maximum values of the photogrametric DSM array. They can be used for feature scaling. Represented as single values expressed in m MSL.

Example visualization of the orthophoto and DSM from the sample is shown in Figure 1.

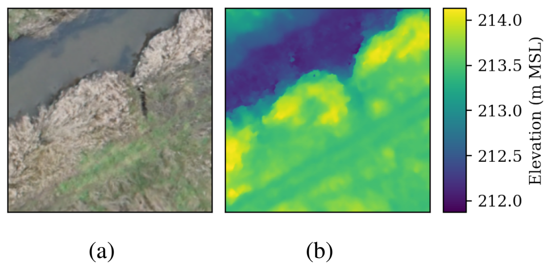

Figure 1: Visualisation of geospatial data from single dataset sample. (a) – photogrammetric orthophoto, (b) – photogrammetric DSM with water surface disturbances.

3 Deep Learning

3.1 Feature scaling

Input data is subjected to feature scaling before it is fed into the model. DSMs values were standardized according to the equation $DSM' = \frac{DSM - \overline{DSM}}{2\sigma}$, where DSM' – standardized sample DSM 2D array with values centered around 0, DSM – raw sample DSM 2D array with values expressed in m MSL, $\overline{DSM}$ – mean value of single subjected DSM array, σ – standard deviation of DSM array pixel values from the entire dataset. This method of standardization has two clear advantages. Firstly, by subtracting the average value of a single subjected sample, standardized DSMs are always centered around zero, so the algorithm sees no difference between samples of the rivers located at regions of different altitudes. The actual water level information is recovered during inverse standardization. Secondly, dividing all samples by the same sigma value of entire dataset, ensures that all standardized samples are scaled equally. It was experimentally found that multiplying the denominator by 2 results in better model accuracy, compared to standardization that does not include this factor. Orthophotos were standardized using Imagenet (Deng et al. [2009]) dataset mean and standard deviation according to the equation $ORT' = \frac{ORT - \mu}{\sigma}$, where ORT' – standardized 3-channel orthophoto RGB image 3D array with values centered around 0, ORT – 3-channel orthophoto RGB image 3D array represented with values from the range [0,1], $\mu = [0.485, 0.456, 0.406]$ – 1D vector containing mean values of each of RGB channels from Imagenet dataset, $\sigma = [0.229, 0.224, 0.225]$ – 1D vector containing standard deviation values of each of RGB channels from Imagenet dataset.

3.2 Models

The model used to create the supervised learning algorithm for determining a single WSE value is based on the VGG-16 architecture (Simonyan and Zisserman [2015]). Several variations of this model have been tested based on neuroevolution architecture search (see section 3.3). The VGG-16 and ResNet were a baseline models.

a VGG-16 Base Model. VGG-16 originally used for image classification was modified to perform single floating point value prediction. The changes made to this model are: i) the input size of the model is 4x256x256. It is a four-channel image in which the first channel contains the DSM and the other three channels are RGB orthophoto channels. ii) After a series of convolution layers, a linear transformation of the array data to a single value was applied. No activation function was used on the model output to obtain a floating point value.

b **Multiresolution VGG-16**. VGG-16 Base Model (**a**) enhanced with multi resolution achieved by concatenation of scaled four-input channels to the output of each max pooling layer.

c **VGG-16 with four CONV blocks** - VGG-16 without last three convolutional layers with changed activation function.

d **VGG-16 with three CONV blocks** - VGG-16 without last six convolutional layers with mutated activation function.

e **VGG-16 with five CONV blocks** - VGG-16 with whole feature extractor.

f **Fine tuned VGG-16** - best pretrained VGG-16 fine tuned by running neuroevolution with weights mutation.

g **ResNet18** - ResNet18 with different convolutional layers configuration.

3.3 Architecture search

Many of recent machine learning works has focused on solutions in which neural network weights are trained through variants of stochastic gradient descent. An alternative approach comes from the field of neuroevolution, which harnesses evolutionary algorithms to optimize neural networks, inspired by the fact that natural brains themselves are the products of an evolutionary process (Faber et al. [2021], Ma et al. [February 2021], Stanley and Miikkulainen [2002], Miikkulainen et al. [Mar 2017], Sun et al. [Oct 2017], E. Galvan [Jun 2020]). In presented work we have set up a neuroevolution based algorithm which can run search through different architectures and modifications of baseline models VGG or ResNet. The sizes of population in our experiments was 16 (eq.1, eq. 2). The number of iterations is in range from 20 to 40. The population is set of the models with different initial random weights ((eq.1, eq. 2)).

$$P = \{F^i_\Theta, \Theta = \{\theta_0, \theta_1, ..., \theta_N\} \wedge i \in \{1, 2, ..., population\_size\}\} \tag{1}$$

$$F^i_\Theta(x) = f^i_{\theta_N}(f^i_{\theta_{N-1}}...(f^i_{\theta_0}(x))) \rightarrow level\_prediction \tag{2}$$

Our implementation consists of mutation operator which can change length of the model F^i_Θ or internal parameters of chosen layer $f^i_{\theta_{l\_id}}$ like number of input channels or kernel size (eq.3, eq.4 and eq.5).

$$m : Parent \times layer\_id \rightarrow Child \tag{3}$$

$$m(F^i_\Theta, l\_id) \rightarrow F^{i'}_\Theta \tag{4}$$

$$F^{i'}_\Theta(x) = f^i_{\theta_N}(f^i_{\theta_{N-1}}...f^{i'}_{\theta_{l\_id}}...(f^i_{\theta_0}(x))) \tag{5}$$

After each iteration the best solutions are chosen and form new generation for the next one. In each iteration models are trained with gradient descent in 5 epochs. Additional step is neuroevolution based fine tuning which run mutation operation on a population of gradient descent pretrained networks and evaluates them on training dataset. Each single mutation perturbates some small percentage of weights (1-2%). Finally, best models are tested on a validation dataset.

4 Results and future works

The results are shown in Tab. 2. The models listed in table are those which were set manually (VGG-16 Base Model, Multiresolution VGG-16 Base Model) and other which were generated by neuroevolution search. In parentheses there are combinations of the number of channels for successive blocks inside the models. In the rows where these numbers are not given, the number of channels in the blocks is the same as in the original version of the model. In It is shown that neuroevolution search improved accuracy of water level prediction. Our fine tuning approach decrease further the prediction error. It is worth to mention that our best deep learning models outperform other manual methods of determining WSE from photogrammetric DSMs and are close to the accuracy of the more complicated and expensive AirSWOT method (Tab. 1). The future work will concentrate on further model exploration using more sophisticated neuroevolution, including Vision Transformer based feature extractor (Dosovitskiy et al. [2020]), ResNeSt (Zhang et al. [2020]) etc. The neuroevolution algorithm will be incorporated with crossover, clustering, hyperparameter optimization (Faber et al. [2021]) and multiresolution options. Especially model topology will be more explored, not only individual layers will be evolved but the internal network topology. Also Bayesian estimation of uncertainty and models sensitivity analysis will be performed (Gal and Ghahramani [2016]).

Table 2: Deep learning models prediction accuracy

Model	RMSE [cm]
Fine tuned VGG, 5 blocks with LeakyReLU	9.89
VGG, 5 blocks with LeakyReLU (66,146,176,222,222)	10.01
VGG, 3 blocks with ReLU	10.44
Multiresolution VGG-16 Base Model	10.50
VGG, 4 blocks with LeakyReLU (84,137,258,497)	11.18
VGG-16 Base Model	11.69
Resnet18 Model (42, 193, 293, 579)	14.13

Acknowledgments The present work has been supported by: the EU project titled: WATERLINE (project id CHIST-ERA-19-CES-006); project WATERLINE supported by the National Science Centre, Poland, under CHIST-ERA IV programme, which has received funding from the EU Horizon 2020 Research and Innovation Programme, under Grant Agreement no 857925 (project id: 2020/02/Y/ST10/00065); the Polish Ministry of Science and Higher Education Project "Initiative for Excellence – Research University"; PLGrid Infrastructure.

Paper checklist

Do the main claims made in the abstract and introduction accurately reflect the paper's contributions and scope? We have made every effort to ensure that the abstract and introduction accurately reflect the paper's contributions and scope.
Have you read the ethics review guidelines and ensured that your paper conforms to them? Yes.
Did you discuss any potential negative societal impacts of your work? No, observations of water levels have been conducted for many years without any noticeable negative societal impact.
Did you describe the limitations of your work? No, however, these are typical limitations of Deep Lerning solutions, such as no guarantee of model performance for data of a different type than used during model training. For this reason, further work is planned to introduce Bayesian uncertainty estimation.
Did you include the code, data, and instructions needed to reproduce the main experimental results (either in the supplemental material or as a URL)? Dataset download link is included in text. Due to text size limitation, detailed information on the replication of the results will be provided in a full-length journal article that is planned to publish within the next 3 months.
Did you specify all the training details (e.g., data splits, hyperparameters, how they were chosen)? Dataset split information is provided in the text. The most important information about the neuroevolutionary algorithm is included in the text.
Did you report error bars (e.g., with respect to the random seed after running experiments multiple times)? No, this is planed for future work of Bayesian uncertainty investigation.
Did you include the amount of compute and the type of resources used (e.g., type of GPUs, internal cluster, or cloud provider)? No, due to text length limitation, this information will be provided in a full-length journal article that is planned to publish within the next 3 months.
If your work uses existing assets, did you cite the creators? Dataset uses data acquired by other researchers and proper citations are included in text and on the dataset website.
Did you mention the license of the assets? No, as this data can be distributed under the Creative Commons Attribution 2.0 Generic license.
Did you include any new assets either in the supplemental material or as a URL? Yes, the dataset.
Did you discuss whether and how consent was obtained from people whose data you're using/curating? No, as this data can be distributed under the Creative Commons Attribution 2.0 Generic license.
Did you discuss whether the data you are using/curating contains personally identifiable information or offensive content? No. The data does not contain such information.

References

Elizabeth H. Altenau, Tamlin M. Pavelsky, Delwyn Moller, Christine Lion, Lincoln H. Pitcher, George H. Allen, Paul D. Bates, Stéphane Calmant, Michael Durand, and Laurence C. Smith. AirSWOT measurements of river water surface elevation and slope: Tanana river, AK. *Geophysical Research Letters*, 44(1):181–189, January 2017. doi: 10.1002/2016gl071577. URL `https://doi.org/10.1002/2016gl071577`.

Filippo Bandini, Tanya Pheiffer Sunding, Johannes Linde, Ole Smith, Inger Klint Jensen, Christian Josef Köppl, Michael Butts, and Peter Bauer-Gottwein. Dataset used in "unmanned aerial system (uas) observations of water surface elevation in a small stream: comparison of radar altimetry, lidar and photogrammetry techniques", 2019. URL `https://zenodo.org/record/3519887`.

Filippo Bandini, Tanya Pheiffer Sunding, Johannes Linde, Ole Smith, Inger Klint Jensen, Christian Josef Köppl, Michael Butts, and Peter Bauer-Gottwein. Unmanned aerial system (UAS) observations of water surface elevation in a small stream: Comparison of radar altimetry, LIDAR and photogrammetry techniques. *Remote Sensing of Environment*, 237:111487, February 2020. doi: 10.1016/j.rse.2019.111487. URL `https://doi.org/10.1016/j.rse.2019.111487`.

Yves Bühler, Marc S. Adams, Andreas Stoffel, and Ruedi Boesch. Photogrammetric reconstruction of homogenous snow surfaces in alpine terrain applying near-infrared UAS imagery. *International Journal of Remote Sensing*, 38(8-10):3135–3158, January 2017. doi: 10.1080/01431161.2016.1275060. URL `https://doi.org/10.1080/01431161.2016.1275060`.

Jia Deng, Wei Dong, Richard Socher, Li-Jia Li, Kai Li, and Li Fei-Fei. ImageNet: A large-scale hierarchical image database. In *2009 IEEE Conference on Computer Vision and Pattern Recognition*. IEEE, June 2009. doi: 10.1109/cvpr.2009.5206848. URL `https://doi.org/10.1109/cvpr.2009.5206848`.

Alessio Domeneghetti. On the use of SRTM and altimetry data for flood modeling in data-sparse regions. *Water Resources Research*, 52(4):2901–2918, April 2016. doi: 10.1002/2015wr017967. URL `https://doi.org/10.1002/2015wr017967`.

Alexey Dosovitskiy, Lucas Beyer, Alexander Kolesnikov, Dirk Weissenborn, Xiaohua Zhai, Thomas Unterthiner, Mostafa Dehghani, Matthias Minderer, Georg Heigold, Sylvain Gelly, Jakob Uszkoreit, and Neil Houlsby. An image is worth 16x16 words: Transformers for image recognition at scale. *CoRR*, abs/2010.11929, 2020. URL `https://arxiv.org/abs/2010.11929`.

P. Mooney E. Galvan. Neuroevolution in deep neural networks: Current trends and future challenges. *CoRR abs/2006.05415*, Jun 2020.

Kamil Faber, Marcin Pietron, and Dominik Zurek. Ensemble neuroevolution-based approach for multivariate time series anomaly detection. *Entropy*, 23(11), November 2021. doi: https://doi.org/10.3390/e23111466.

Yarin Gal and Zoubin Ghahramani. Dropout as a bayesian approximation: Representing model uncertainty in deep learning, 2016.

IPCC. *Climate change 2014 : synthesis report*. Intergovernmental Panel on Climate Change, Geneva, Switzerland, 2015. ISBN 978-92-9169-143-2.

Abdollah Asadzadeh Jarihani, John Nikolaus Callow, Kasper Johansen, and Ben Gouweleeuw. Evaluation of multiple satellite altimetry data for studying inland water bodies and river floods. *Journal of Hydrology*, 505:78–90, November 2013. doi: 10.1016/j.jhydrol.2013.09.010. URL `https://doi.org/10.1016/j.jhydrol.2013.09.010`.

L. Javernick, J. Brasington, and B. Caruso. Modeling the topography of shallow braided rivers using structure-from-motion photogrammetry. *Geomorphology*, 213:166–182, May 2014. doi: 10.1016/j.geomorph.2014.01.006. URL `https://doi.org/10.1016/j.geomorph.2014.01.006`.

E. Kasvi, J. Salmela, E. Lotsari, T. Kumpula, and S.N. Lane. Comparison of remote sensing based approaches for mapping bathymetry of shallow, clear water rivers. *Geomorphology*, 333:180–197, May 2019. doi: 10.1016/j.geomorph.2019.02.017. URL `https://doi.org/10.1016/j.geomorph.2019.02.017`.

Jakub Langhammer, Jana Bernsteinová, and Jakub Miřijovský. Building a high-precision 2d hydrodynamic flood model using UAV photogrammetry and sensor network monitoring. *Water*, 9(11):861, November 2017. doi: 10.3390/w9110861. URL `https://doi.org/10.3390/w9110861`.

Richard Lawford, Adrian Strauch, David Toll, Balazs Fekete, and Douglas Cripe. Earth observations for global water security. *Current Opinion in Environmental Sustainability*, 5(6):633–643, December 2013. doi: 10.1016/j.cosust.2013.11.009. URL `https://doi.org/10.1016/j.cosust.2013.11.009`.

A. Ma, Y. Wan, Y. Zhong, and J. Wang. Scenenet: Remote sensing scene classification deep learning network using multi-objective neural evolution architecture search. *ISPRS Journal of Photogrammetry and Remote Sensing pp. 171-188*, DOI:10.1016/j.isprsjprs.2020.11.025, February 2021.

Matthew F. McCabe, Matthew Rodell, Douglas E. Alsdorf, Diego G. Miralles, Remko Uijlenhoet, Wolfgang Wagner, Arko Lucieer, Rasmus Houborg, Niko E. C. Verhoest, Trenton E. Franz, Jiancheng Shi, Huilin Gao, and Eric F. Wood. The future of earth observation in hydrology. *Hydrology and Earth System Sciences*, 21(7):3879–3914, July 2017. doi: 10.5194/hess-21-3879-2017. URL https://doi.org/10.5194/hess-21-3879-2017.

R. Miikkulainen, J. Liang, E. Meyerson, A. Rawal, D. Fink, O. Francon, B. Raju, H. Shahrzad, A. Navruzyan, N. Duffy, and B. Hodjat. Evolving deep neural networks. *CoRR abs/1703.00548*, Mar 2017.

V. Montesarchio, F. Napolitano, M. Rianna, E. Ridolfi, F. Russo, and S. Sebastianelli. Comparison of methodologies for flood rainfall thresholds estimation. *Natural Hazards*, 75(1):909–934, August 2014. doi: 10.1007/s11069-014-1357-3. URL https://doi.org/10.1007/s11069-014-1357-3.

Mohamar Moussa Ouédraogo, Aurore Degré, Charles Debouche, and Jonathan Lisein. The evaluation of unmanned aerial system-based photogrammetry and terrestrial laser scanning to generate DEMs of agricultural watersheds. *Geomorphology*, 214:339–355, June 2014. doi: 10.1016/j.geomorph.2014.02.016. URL https://doi.org/10.1016/j.geomorph.2014.02.016.

H. Pai, H. F. Malenda, M. A. Briggs, K. Singha, R. González-Pinzón, M. N. Gooseff, and S. W. Tyler and. Potential for small unmanned aircraft systems applications for identifying groundwater-surface water exchange in a meandering river reach. *Geophysical Research Letters*, 44(23), December 2017. doi: 10.1002/2017gl075836. URL https://doi.org/10.1002/2017gl075836.

Tamlin M. Pavelsky, Michael T. Durand, Konstantinos M. Andreadis, R. Edward Beighley, Rodrigo C.D. Paiva, George H. Allen, and Zachary F. Miller. Assessing the potential global extent of SWOT river discharge observations. *Journal of Hydrology*, 519:1516–1525, November 2014. doi: 10.1016/j.jhydrol.2014.08.044. URL https://doi.org/10.1016/j.jhydrol.2014.08.044.

Karen Simonyan and Andrew Zisserman. Very deep convolutional networks for large-scale image recognition, 2015.

Kenneth O. Stanley and Risto Miikkulainen. Evolving neural networks through augmenting topologies. *Evolutionary Computation*, 10(2):99–127, 2002. doi: 10.1162/106365602320169811.

Yanan Sun, Bing Xue, Mengjie Zhang, and Gary G. Yen. Evolving deep convolutional neural networks for image classification. *CoRR abs/1710.10741*, Oct 2017.

Radosław Szostak, Mirosław Zimnoch, Przemysław Wachniew, Paweł Ćwiąkała, and Marcin Pietroń. DSM water level: An UAV photogrammetry dataset for determination of river surface level using machine learning, 2021. URL https://zenodo.org/record/5257183.

Angelica Tarpanelli, Silvia Barbetta, Luca Brocca, and Tommaso Moramarco. River discharge estimation by using altimetry data and simplified flood routing modeling. *Remote Sensing*, 5(9):4145–4162, August 2013. doi: 10.3390/rs5094145. URL https://doi.org/10.3390/rs5094145.

UNESCO. *The United Nations world water development report 2020: water and climate change*. United Nations Educational, Scientific and Cultural Organization, Paris, 2020. ISBN 978-92-3-100371-4.

Mercedes Vélez-Nicolás, Santiago García-López, Luis Barbero, Verónica Ruiz-Ortiz, and Ángel Sánchez-Bellón. Applications of unmanned aerial systems (UASs) in hydrology: A review. *Remote Sensing*, 13(7):1359, April 2021. doi: 10.3390/rs13071359. URL https://doi.org/10.3390/rs13071359.

A. S. Woodget, P. E. Carbonneau, F. Visser, and I. P. Maddock. Quantifying submerged fluvial topography using hyperspatial resolution UAS imagery and structure from motion photogrammetry. *Earth Surface Processes and Landforms*, 40(1):47–64, August 2014. doi: 10.1002/esp.3613. URL https://doi.org/10.1002/esp.3613.

Hang Zhang, Chongruo Wu, Zhongyue Zhang, Yi Zhu, Zhi Zhang, Haibin Lin, Yue Sun, Tong He, Jonas Mueller, R. Manmatha, Mu Li, and Alexander J. Smola. Resnest: Split-attention networks. *CoRR*, abs/2004.08955, 2020. URL https://arxiv.org/abs/2004.08955.